JACS
JOURNAL OF THE AMERICAN CHEMICAL SOCIETY
pubs.acs.org/JACS
Article

18-Crown-6 Coordinated Metal Halides with Bright Luminescence and Nonlinear Optical Effects

Elena Merzlyakova, Silke Wolf, Sergei Lebedkin, Lkhamsuren Bayarjargal, B. Lilli Neumeier, Daniel Bartenbach, Christof Holzer, Wim Klopper, Bjoern Winkler, Manfred Kappes, and Claus Feldmann*

Cite This: J. Am. Chem. Soc. 2021, 143, 798−804

Read Online

ACCESS | Metrics & More | Article Recommendations | Supporting Information

ABSTRACT: The crown-ether coordination compounds ZnX_2(18-crown-6), EuX_2(18-crown-6) (*X*: Cl, Br, I), MnI_2(18-crown-6), Mn_3Cl_6(18-crown-6)$_2$, Mn_3I_6(18-crown-6)$_2$, and Mn_2I_4(18-crown-6) are obtained by ionic-liquid-based synthesis. Whereas MX_2(18-crown-6) (*M*: Zn, Eu) show conventional structural motives, Mn_3Cl_6(18-crown-6)$_2$, Mn_3I_6(18-crown-6)$_2$, and Mn_2I_4(18-crown-6) exhibit unusual single MnX_4 tetrahedra coordinated to the crown-ether complex. Surprisingly, some compounds show outstanding photoluminescence. Thus, rare Zn^{2+}-based luminescence is observed and unexpectedly efficient for ZnI_2(18-crown-6) with a quantum yield of 54%. Unprecedented quantum yields are also observed for Mn_3I_6(18-crown-6)$_2$, $EuBr_2$(18-crown-6), and EuI_2(18-crown-6) with values of 98, 72, and 82%, respectively, which can be rationalized based on the specific structural features. Most remarkable, however, is Mn_2I_4(18-crown-6). Its specific structural features with finite sensitizer−activator couples result in an extremely strong emission with an outstanding quantum yield of 100%. Consistent with its structural features, moreover, anisotropic angle-dependent emission under polarized light and nonlinear optical (NLO) effects occur, including second-harmonic generation (SHG). The title compounds and their optical properties are characterized by single-crystal structure analysis, X-ray powder diffraction, chemical analysis, density functional theory (DFT) calculations, and advanced spectroscopic methods.

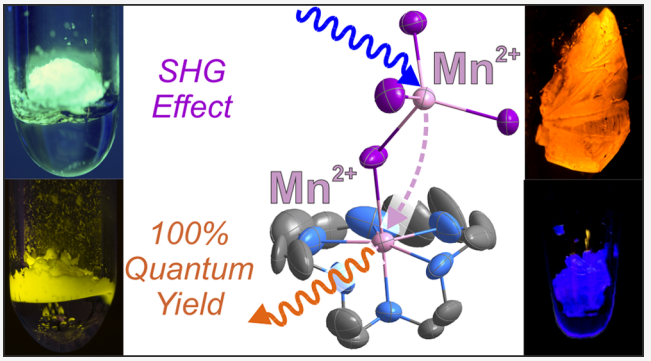

1. INTRODUCTION

Crown ethers, discovered by Pedersen,[1] are known as unique ligands in regard of many aspects.[2] Today, they are available with different ring-opening diameters (e.g., 120−150 pm for 12-crown-4, 450−500 pm for 24-crown-8), and they can contain different heteroatoms such as oxygen, sulfur, or nitrogen as coordinating sites.[2] In inorganic and metal−organic chemistry, crown ethers are known to coordinate almost all types of metal cations. Because of their strong chelating effect and adaptable ring-openings, even alkali metal cations can be strongly bound.[2] Moreover, fascinating compounds were realized with crown ethers as ligands, including, for instance, alkali metal alkalides and electrides,[3] phase-transfer reagents,[4] or low-coordinated nitrogen complexes.[5] 18-Crown-6 is perhaps the most widely applied crown ether. Because of its ring-opening diameter (∼300 pm), 18-crown-6 is especially known for optimal coordination of K^+ (*r*: 138 pm).[6]

In contrast to the rich coordination chemistry, little is known about the photoluminescence (PL) of crown-ether coordination compounds. PL was predominately reported for crown ethers substituted with specific fluorescent dyes (anthracenes, pyrenes, etc.).[7] Such dye-substituted systems were widely explored for sensing and analytical chemistry to detect the presence of certain metal cations.[7,8] Knowledge on metal-based luminescence of crown-ether coordination compounds is rare and has only been reported for complexes of Sm^{2+}, $Eu^{2+/3+}$, and Tm^{2+} with low intensity and/or only at low temperatures (≤77 K).[9]

With this work, we could realize a great number of novel 18-crown-6 coordinated metal halides by reacting the divalent metal halides ZnX_2, EuX_2, and MnX_2 (*X*: Cl, Br, I) with 18-crown-6 in ionic liquids. Surprisingly, some of these crown-ether compounds show unprecedented luminescence features, including rare Zn^{2+}-based luminescence, extremely efficient emission with quantum yields up to 100%, and nonlinear optical (NLO) effects.

Received: September 2, 2020
Published: January 6, 2021

https://dx.doi.org/10.1021/jacs.0c09454
J. Am. Chem. Soc. 2021, 143, 798−804

2. EXPERIMENTAL SECTION

Chemicals. All sample handling was performed with Schlenk techniques under argon or in argon-filled gloveboxes (MBraun Unilab, O_2/H_2O < 1 ppm). All reactions were performed by using standard Schlenk techniques and glass ampules. All glassware was evacuated three times ($<10^{-3}$ mbar) prior to use, heated, and flushed with argon to remove moisture.

General Synthesis. All title compounds were prepared by reacting the respective metal halides MX_2 (*M*: Zn, Eu, Mn; *X*: Cl, Br, I) and 18-crown-6 in the ionic liquid ($[(n\text{-Bu})_3\text{MeN}][\text{N(Tf)}_2]$ or $[\text{EMIm}][\text{NTf}_2]$) at 80−150 °C for 3 weeks in sealed, argon-filled glass ampules. In the case of the iodides, the addition of minor amounts of the Lewis acid SnI_4 promotes the growth of single crystals. In alternative to the ionic-liquid-based synthesis, some title compounds can be also obtained by direct reaction of MX_2 and 18-crown-6. Generally, the ionic liquid promotes the formation of single crystals, whereas the direct synthesis results in microcrystalline powder samples. More details can be found in the Supporting Information.

Structure analysis based on single crystals and powder diffraction with Rietveld refinement is described in detail in the Supporting Information. Moreover, details related to infrared spectroscopy, thermogravimetry, energy-dispersive X-ray spectroscopy, and elemental analysis can be also found in the Supporting Information.

PL Spectroscopy. A Horiba Jobin Yvon Spex Fluorolog 3.2 spectrometer was used to obtain excitation and emission spectra of powder samples. The spectrometer was equipped with a 450 W xenon lamp and double grating excitation/emission monochromators as well as a photomultiplier as detector.

The absolute PL quantum yield was determined according to ref 10. Briefly, the ratio of photons emitted and absorbed by a solid sample—resulting in the quantum yield—was measured by using an integrating sphere. The method comprises measurements at two sample positions inside the sphere (or at two different directions of the excitation light beam as realized in the Fluorolog) with direct and indirect illumination of the sample, which improves the accuracy.

Polarized emission measurements were performed with a setup based on a WiTec CRM200 Raman microscope by using a linearly polarized diode laser at 372 nm for excitation and a piezo-driven linear polarizer placed in the emission-light beam to probe its polarization. To avoid degradation in air, the sample was measured in a gastight optical cell assembled in an argon glovebox.

Second harmonic generation (SHG) measurements were performed with powder samples according to the Kurtz−Perry method. An optical parametric oscillator pumped with 355 nm was used to generate the fundamental pump waves between 960 and 1400 nm in steps of 20 nm. Second harmonic signals with wavelengths between 480 and 700 nm were separated by using a short-pass filter and detected by using a spectrometer. The setup is described in detail in the Supporting Information.

3. RESULTS AND DISCUSSION

Synthesis and Structural Characterization. All title compounds were prepared by heating the respective divalent metal halide and the crown ether at mild temperature (80−150 °C) for 1−3 weeks in the ionic liquid (Figure 1). The ionic liquid, on the one hand, supports the dissolution of the metal halides and, on the other hand, serves as an inert solvent.[11] In regard to the optical properties, it is particularly important that the solvent does not coordinate the dissolved metal cations and that it does not form coordination compounds itself under the selected conditions. Whereas the ionic-liquid-based synthesis turned out to be optimal for crystal growth, microcrystalline powder samples can be also prepared for some compounds via direct reaction of MX_2 and 18-crown-6 (Supporting Information).

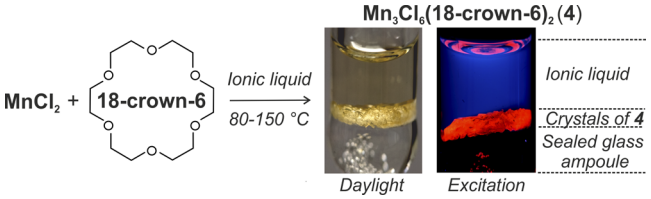

Figure 1. Ionic-liquid-based synthesis of MX_2/18-crown-6 compounds with Mn_3Cl_6(18-crown-6)$_2$ as example (photos show argon-filled glass ampules after the reaction).

The structures of all title compounds were determined by X-ray structure analysis based on single crystals (Table 1, Tables S1−S12, and Figures S1−S11). Structure, chemical composition, and purity were further confirmed by X-ray powder diffraction analysis with Rietveld refinement as well as by infrared spectroscopy, thermogravimetry, energy-dispersive X-ray spectroscopy, and elemental analysis (Tables S13−S15 and Figures S12−S17).

The structural features of the title compounds are primarily influenced by the size of the cation in relation to the ring-opening of 18-crown-6. The resulting coordination and connectivity also have major impact on the PL properties (Tables 1 and 2). In this regard, the comparison of all title compounds is indicative for the special situation of some crown-ether coordination compounds such as Mn_2I_4(18-crown-6) (**7**). First of all, ZnX_2(18-crown-6) and EuX_2(18-crown-6) (*X*: Cl, Br, I) show simple molecular arrangements with the metal cation equatorially coordinated by the crown ether and two halide atoms on the axial positions (Figure 2; Figures S1−S3 and S8−S10). The Zn−*X* and Eu−*X* distances are well in agreement with the respective binary metal halides ZnX_2 and EuX_2 (Table S12). For Zn^{2+} as the smallest cation (*r*: 74 pm),[12] a noncentric coordination with three shorter and three longer Zn−O distances is observed. This results in a disordered location of Zn^{2+} over three equal positions for **1** and **2** (Figure 2a), which is still in accordance with the rhomboedral lattice symmetry. The large Eu^{2+} (*r*: 117 pm),[12] in contrast, shows ideal centric coordination of the cation (Figure 2b) but partially with dislocation of the crown-ether molecule (Figure S10).

In contrast to the conventional structures of the Zn^{2+}- and Eu^{2+}-based compounds, structure and coordination of the Mn^{2+} compounds are more complex (Figure 2). Mn_3Cl_6(18-crown-6)$_2$ and Mn_3I_6(18-crown-6)$_2$ consist of $[MnX(\text{18-crown-6})]^+$ cations and $[MnX(\text{18-crown-6})MnX_4]^-$ anions (Figure 2c; Figures S4 and S5). In the $[MnX(\text{18-crown-6})]^+$ cation, Mn^{2+} is coordinated by all six oxygen atoms of a significantly bent crown-ether molecule and a single chlorine/iodine atom. In the $[MnX(\text{18-crown-6})MnCl_4]^-$ anion, Mn^{2+} is coordinated only by five oxygen atoms of 18-crown-6 as well as by two chlorine or iodine atoms, one of them bridging to a single MnX_4 tetrahedron. Such coordination and structure were also observed for Mn_3Br_6(18-crown-6)$_2$.[13] MnI_2(18-crown-6) is comparable to the Zn^{2+}/Eu^{2+}-containing compounds with the exception of only five oxygen atoms of 18-crown-6 being coordinated to Mn^{2+} (Figure S6). The sixth oxygen atom remains uncoordinated, which is of course unusual for chelating ligands. Mn_2I_4(18-crown-6), finally, contains Mn^{2+} coordinated by six oxygen atoms of a significantly bent crown-ether molecule as well as by a bridging iodine atom, which represents the corner of a MnI_4 tetrahedron (Figure 2d and Figure S7). The observed different

https://dx.doi.org/10.1021/jacs.0c09454
J. Am. Chem. Soc. 2021, 143, 798−804

Table 1. Comparison of the Crystallographic Data of All Title Compounds

compound	space group	lattice parameters			
		a (pm)	*b* (pm)	*c* (pm)	*β* (deg)
$ZnCl_2$(18-crown-6) (**1**)	*R*3	1123.4(3)	1123.4(3)	1195.9(5)	
$ZnBr_2$(18-crown-6) (**2**)	*R*3	1154.4(2)	1154.4(2)	1193.4(2)	
ZnI_2(18-crown-6) (**3**)	*Pnma*	1607.2(5)	2803.1(1)	829.6(2)	
Mn_3Cl_6(18-crown-6)$_2$ (**4**)	$P2_1/c$	1667.0(3)	1064.2(2)	2579.8(8)	124.6(1)
Mn_3I_6(18-crown-6)$_2$ (**5**)	$P2_1/n$	1710.2(3)	1125.2(2)	2274.8(5)	91.9(1)
MnI_2(18-crown-6) (**6**)	*C*2/*c*	1087.1(2)	1201.0(2)	2851.4(6)	94.4(1)
Mn_2I_4(18-crown-6) (**7**)	$P2_12_12_1$	1148.9(2)	1307.5(3)	1643.7(3)	
$EuCl_2$(18-crown-6) (**8**)	*R*3	1155.2(2)	1155.2(2)	1199.7(2)	
$EuBr_2$(18-crown-6) (**9**)	*R*3	1192.9(2)	1192.9(2)	1192.5(2)	
EuI_2(18-crown-6) (**10**)	*C*2/*m*	1296.2(3)	1088.3(2)	802.8(2)	120.3(1)
SrI_2(18-crown-6) (**11**)	*C*2/*m*	1299.6(3)	1086.4(3)	805.0(2)	119.9(3)

Table 2. Comparison of the PL Features of All Title Compounds

compound	excitation λ_{max} (nm)	emission λ_{max} (nm)	quantum yield[a] (%)
$ZnCl_2$(18-crown-6) (**1**)	368, 445	535	22(4)
$ZnBr_2$(18-crown-6) (**2**)	370	470	<5
ZnI_2(18-crown-6) (**3**)	348	517	54(3)
Mn_3Cl_6(18-crown-6)$_2$ (**4**)	356, 407, 431, 444, 512	611	20(4)
Mn_3I_6(18-crown-6)$_2$ (**5**)	320, 450, 423, 509	605	98(3)
MnI_2(18-crown-6) (**6**)	327, 337, 368, 407, 423, 509	563	16(3)
Mn_2I_4(18-crown-6) (**7**)	312, 346, 371, 474	605	100(3)
$EuCl_2$(18-crown-6) (**8**)	397	414	36(4)
$EuBr_2$(18-crown-6) (**9**)	398	415	72(3)
EuI_2(18-crown-6) (**10**)	370	414	82(3)
SrI_2(18-crown-6) (**11**)	398	477	<5

[a]Quantum yield measured at room temperature.

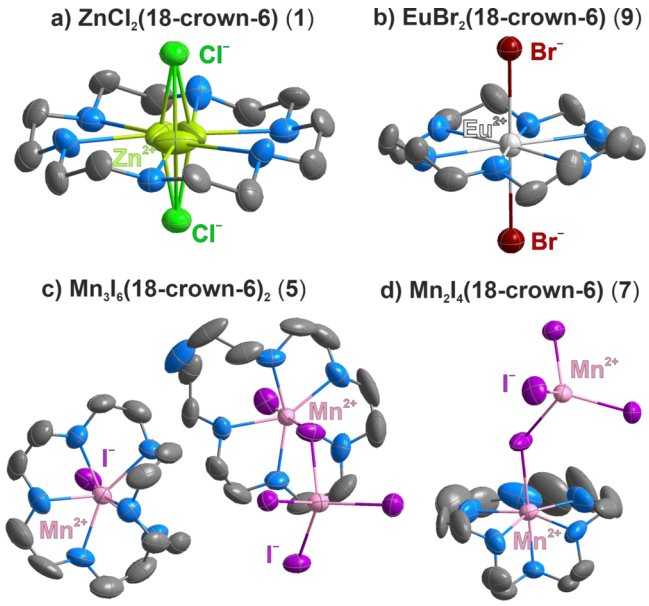

Figure 2. Exemplary structural features of MX_2/18-crown-6 compounds: (a) $ZnCl_2$(18-crown-6) (with disordered Zn^{2+}); (b) $EuBr_2$(18-crown-6); (c) Mn_3I_6(18-crown-6)$_2$ with $[MnI(18\text{-crown-}6)]^+$ cation and $[Mn_2I_4(18\text{-crown-}6)]^-$ anion; (d) Mn_2I_4(18-crown-6).

structural features can be attributed to the mismatch between the radius of Mn^{2+} (*r*: 83 pm) and the ring-opening of 18-crown-6 (about 300 pm). Mn^{2+} is neither small enough to clearly prefer off-center (3 + 3) coordination (like Zn^{2+}) nor large enough for central coordination (like Eu^{2+}).

Although 18-crown-6 is a well-known ligand, coordination compounds with Eu^{2+} [9c,d] and especially with Mn^{2+} and Zn^{2+} are rare. Compounds such as $[K(18\text{-crown-}6)][Mn_4(ThiaSO_2)_2F]$ ($ThiaSO_2$ = *p-tert*-butylsulfonylcalix[4]-arene), $[K(18\text{-crown-}6)]_4[(MnBr_4)(TlBr_4)_2]$, or $[H_3O(18\text{-crown-}6)]_2[MnBr_4]$ contain 18-crown-6, which, however, coordinates K^+ or H_3O^+ instead of Mn^{2+}.[14] The coordination of Zn^{2+} with 18-crown-6 typically includes H_2O as additional ligand (e.g., $[ZnCl(H_2O)(18\text{-crown-}6)]_2[Zn_2Cl_6]$, $[ZnCl_2(H_2O)(18\text{-crown-}6)]$).[15] For compounds with OH-containing ligands coordinated to the metal, PL is typically excluded due to vibronic quenching. Because of the mismatch of the ring-opening of 18-crown-6 and the size of the cation, Zn^{2+} and Mn^{2+} were preferably coordinated by the smaller crown ethers 15-crown-5 and 12-crown-4.[9c,14c,15c,16c]

Photoluminescence Features. Surprisingly, the 18-crown-6 coordinated metal halides show outstanding luminescence properties, which can be directly correlated to their specific structural features (Figure 3, Table S16, and Figures S18−S30). First of all, the emission of Zn^{2+} is unexpected anyway (Figure 3a). Zn^{2+} is typically known as a "PL inactive" host cation and widely used to establish Mn^{2+}-driven emission after partial exchange of Zn^{2+} by Mn^{2+} (e.g., Zn_2SiO_4:Mn^{2+} with 5 mol % Mn^{2+}).[17] Moreover, Zn^{2+} was reported to influence the luminescence of aromatic ligands, but without being involved in the luminescence process itself.[19] Zn^{2+}-driven PL was reported rarely at low temperature and ascribed to $3d^{10}4p^0 \rightarrow 3d^94p^1$ or charge-transfer transitions.[17] In ZnX_2(18-crown-6), 18-crown-6 can be considered as an "innocent" ligand, which excludes the crown ether from being the origin of the PL. This was also verified by SrI_2(18-crown-6) showing only negligible defect-related PL (Table 2; Figures S11 and S30). Besides the surprising PL as such, the efficient Zn^{2+}-based PL of ZnI_2(18-crown-6) (**3**) with a

https://dx.doi.org/10.1021/jacs.0c09454
J. Am. Chem. Soc. 2021, 143, 798−804

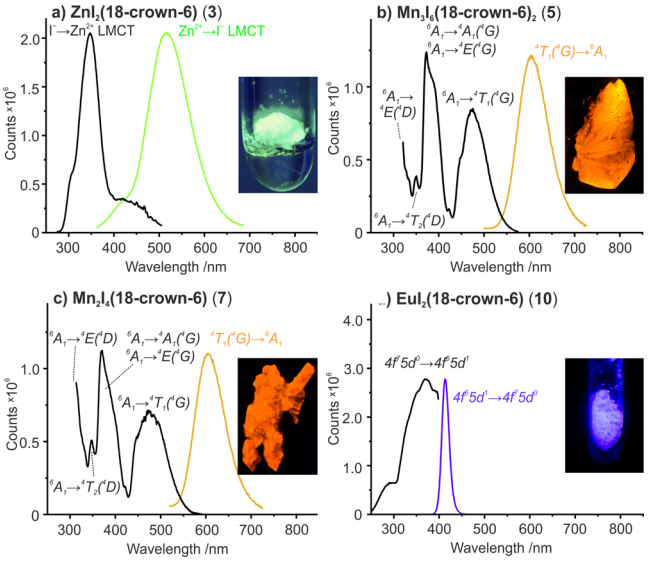

Figure 3. Excitation and emission spectra of selected MX_2/18-crown-6 compounds with photos of powders/crystals under excitation (assignment of transitions according to ref 17b).

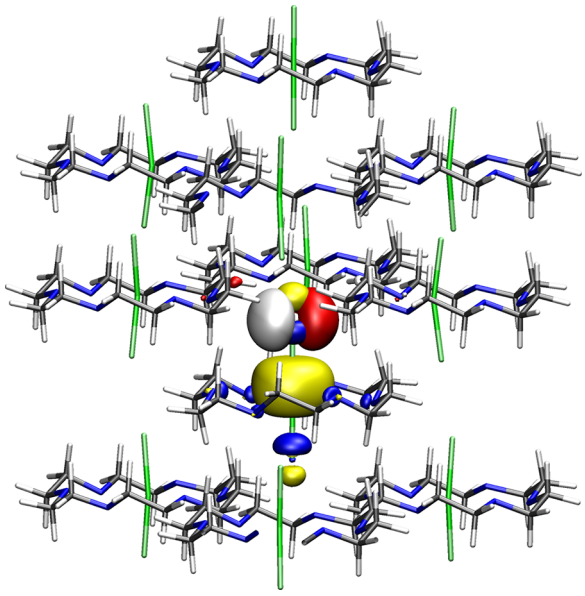

Figure 4. DFT calculation for $ZnCl_2$(18-crown-6) (**1**) with an assembly of 11 molecules showing the electronic excitation from a Cl 3p orbital (red/white: electron donor) to a Zn 4s orbital (blue/yellow: electron acceptor).

quantum yield of 54% is even more remarkable and, to the best of our knowledge, reported here for the first time.

To understand the nature of the Zn^{2+}-based luminescence, we have performed computational studies with density functional theory (DFT) and time-dependent density functional theory (TD-DFT) calculations on single molecules of ZnX_2(18-crown-6) (Supporting Information). It soon turned out that the first singlet excited state for all three compounds ZnX_2(18-crown-6) (X: Cl, Br, I) is characterized by a charge-transfer excitation from a halide np orbital (n = 3, 4, 5, respectively) to the empty 4s orbital of the Zn^{2+} ion. It also turned out that the molecule in its first singlet excited state decomposes. Thus, the halide ion from which the excitation had taken place (which after the excitation formally had become a neutral halogen atom) moves away from the rest of the molecule (Table S17 and Figures S31−S33). Such photodecomposition was observed at various levels of TD-DFT computations as well as at the coupled-cluster level in the CC2 approximation. Because computations on the level of individual molecules were not helpful, assemblies of molecules were investigated that are arranged as in the respective crystal structure (Supporting Information). As a result, the PL observed for ZnX_2(18-crown-6) in the solid state is due to an excited state that can be characterized as a charge-transfer state with an electron transferred from a halide np orbital to an empty 4s orbital of the Zn^{2+} ion, where in the excited state the Zn−X bond distance is larger by 20−30% compared to the ground state (Figures S34−S39). This situation is exemplarily illustrated for $ZnCl_2$(18-crown-6) (**1**) showing the first singlet excited state with the 3p orbital of the chlorine atom and the 4s orbital of the zinc atom involved (Figure 4). In the singlet excited state, the Zn−Cl bond is elongated by 29.5% compared to the ground state.

Mn^{2+} and Eu^{2+} are known as some of the most efficient luminescence centers at all if they are located in a suitable coordinating environment.[17] Thus, commercial lamp and display phosphors such as Zn_2SiO_4:Mn^{2+}, $BaMgAl_{10}O_{17}$:Eu^{2+}, Mn^{2+}, $Sr_3Si_5N_8$:Eu^{2+}, and $Sr[LiAl_3N_4]$:Eu^{2+} show bright PL with quantum yields of 80−90%.[17,18] The Eu^{2+}- and Mn^{2+}-based crown-ether coordination compounds fortunately also show bright PL and the characteristic d−d and f−d transitions of Mn^{2+} and Eu^{2+}, respectively (Figure 3b−d and Figures S23−S29). Surprisingly, the quantum yields even outperform long-optimized commercial phosphors. Thus, EuI_2(18-crown-6) (**10**), Mn_3I_6(18-crown-6)$_2$ (**5**), and Mn_2I_4(18-crown-6) (**7**) exhibit unprecedented quantum yields of 82, 98, and 100% at ambient temperature (Table 2). Efficient PL processes and bright emission at ambient temperature are also confirmed by short decay times in the 0.1−1.0 μs range (Table S16).

The excellent PL performance can be directly correlated to the structural situation, including the rigid coordination of Mn^{2+} and Eu^{2+} by the crown ether, the large distance between the luminescent centers, and the absence of high-energy vibronic states (e.g., O−H). In particular, strongly bent 18-crown-6 molecules as in compounds **4**, **5**, and **7** are obviously most adequate in terms of rigid coordination. As a result, nonemissive loss processes like concentration quenching or thermal quenching are prevented. Vibronic relaxation processes are lowest for heavy iodine, which is why the iodides show the highest quantum yields. Especially Mn_2I_4(18-crown-6) (**7**) has additional advantages with finite sensitizer−activator couples and a defined short distance between the Mn^{2+} pairs (Mn^{2+} ↔ Mn^{2+}: 519(1) pm) and significantly longer distances between different couples (>800 pm) (Figure 5a and Figure S40). Moreover, the noninversion symmetric sites of the tetrahedral $MnI_{1/2}I_{3/1}$ sensitizer as well as of the $MnI_{1/2}$(18-crown-6) activator weaken the parity selection rule and favor highly efficient PL processes (Table 2).

Nonlinear Optical Properties. With regard to the PL properties, Mn_2I_4(18-crown-6) (**7**) is even more interesting due to its polar, chiral space-group symmetry ($P2_12_12_1$) (Table 1). From about 20 single crystals, however, all turned out to be inversion twins with a ratio of the enantiomeric domains close to 50:50 within the significance of the experiment (highest deviation with 43±6 : 57±6), which indicates only a small excess of one crystal enantiomer. Laser microscopy with

https://dx.doi.org/10.1021/jacs.0c09454
J. Am. Chem. Soc. 2021, 143, 798−804

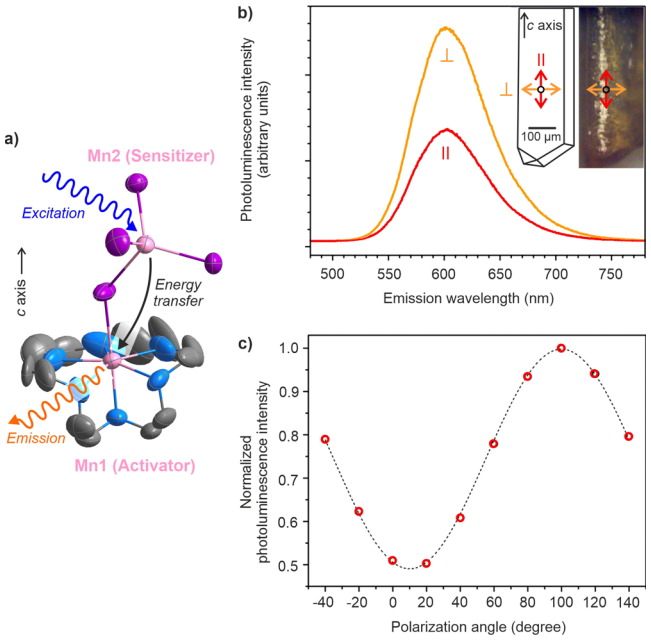

Figure 5. Photoluminescence of Mn_2I_4(18-crown-6) (7) under polarized light. (a) Scheme illustrating the PL process with the finite sensitizer−activator couple. (b) Polarized emission spectra of single crystal (scheme and bright-field image as an inset) excited at 372 nm and recorded with the analyzer axis parallel and perpendicular to the long crystal axis (yellow/red arrows indicate the polarization of the excitation laser beam). (c) Emission intensity at 600 nm as a function of the analyzer rotation angle, Θ (0° corresponds to parallel orientation), with fit to $\cos^2$ Θ variation (dashed curve).

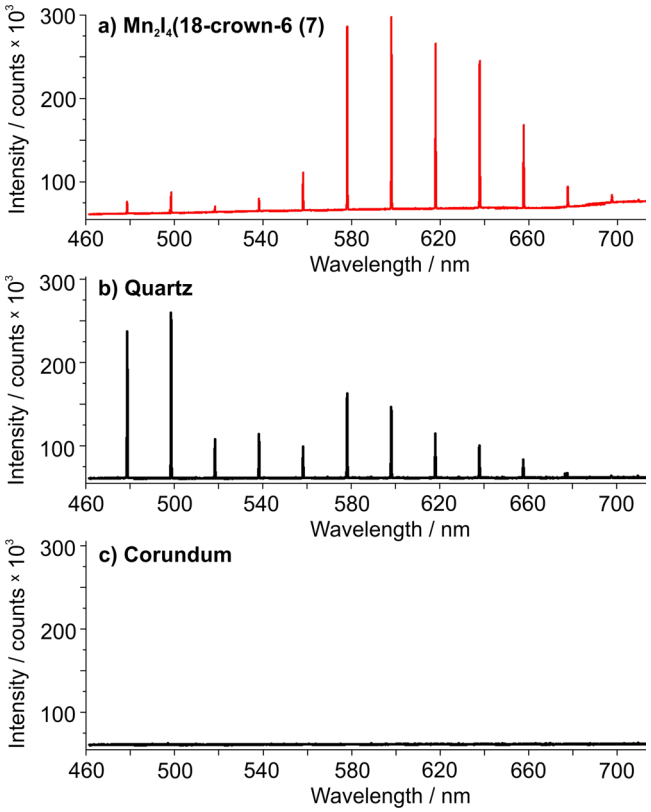

Figure 6. SHG measurement of powder samples: (a) Mn_2I_4(18-crown-6) (7), (b) quartz as a noncentrosymmetric reference, and (c) corundum as a centrosymmetric reference (data after subtraction of cosmic background radiation).

polarized light nevertheless shows a predominant linear emission polarization perpendicular to the long axis of a single crystal (crystallographic *c*-axis; Figure 5b,c and Figure S41). The ratio of this component to that polarized parallel to the long axis amounts to 2. This emission polarization was found to be insensitive to the excitation geometry (with polarization direction of the laser excitation beam either parallel or perpendicular to the long crystal axis). Moreover, the polarized emission intensity is well described by a $\cos^2$ Θ law, where Θ is the rotation angle of the linear polarizer relative to the long crystal axis (Figure 5c). This finding can be again attributed to the specific structural features of Mn_2I_4(18-crown-6) (7) with both well-separated sensitizer−activator couples and highly anisotropic sites of sensitizer ($MnI_{1/2}I_{3/1}$ tetrahedron) and activator ($MnI_{1/2}$(18-crown-6)) (Figure 5a).[17] In the crystal, the $MnI_{1/2}$(18-crown-6) emitters are oriented with the 18-crown-6 units roughly perpendicular to the long crystal axis, thus correlating with the emission anisotropy.

Upon excitation with laser light (960−1400 nm in steps of 20 nm), furthermore, Mn_2I_4(18-crown-6) (7) shows second harmonic signals with wavelengths of 480−700 nm (Figure 6 and Figure S42). Similar to the quartz reference, emission at half of the excitation wavelength is clearly visible. This observation also points to incomplete inversion twinning and a nonlinear optical effect that would be even significantly stronger for enantiopure crystals. Moreover, it needs to be noticed that SHG emission decreases below 580 nm due to Mn^{2+}-driven absorption (Figure 3c). Noteworthy, excitation of 7 at 960−1160 nm results in orange emission peaking at 605 nm due to SHG-driven excitation at 480−580 nm and the efficient PL process. Such an effect is rare and could be promising for optoelectronic applications.

4. CONCLUSIONS

In summary, the crown-ether coordination compounds ZnX_2(18-crown-6) and EuX_2(18-crown-6) (*X*: Cl, Br, I) as well as Mn_3Cl_6(18-crown-6)$_2$, Mn_3I_6(18-crown-6)$_2$, MnI_2(18-crown-6), and Mn_2I_4(18-crown-6) were prepared by ionic-liquid-based synthesis. The structural features of the title compounds are primarily influenced by the size of the cation in relation to the ring-opening of 18-crown-6 (about 300 pm). In this regard, Mn^{2+} (*r*: 83 pm) is neither small enough to clearly prefer off-center (3 + 3) coordination (like Zn^{2+}, *r*: 74 pm) nor large enough for central coordination (like Eu^{2+}, *r*: 117 pm). As a result, Mn_3Cl_6(18-crown-6)$_2$, Mn_3I_6(18-crown-6)$_2$, and Mn_2I_4(18-crown-6) exhibit unusual single MnX_4 tetrahedra coordinated to the crown-ether complex.

The structural features of the crown-ether coordination compounds also have major impact on the optical properties. First of all, unexpected emission of all Zn^{2+}-containing compounds was observed and could be attributed by computation to charge-transfer transition between the halide *n*p orbital and the zinc 4s orbital. Besides the surprising PL as such, ZnI_2(18-crown-6) shows a remarkable quantum yield of 54%, which is the highest value observed for Zn^{2+}-based PL. The Mn^{2+}- and Eu^{2+}-containing crown-ether coordination compounds show bright PL with the characteristic d−d (Mn^{2+}) and f−d transitions (Eu^{2+}). Surprisingly, the PL efficiency of Mn_3Cl_6(18-crown-6)$_2$, Mn_3I_6(18-crown-6)$_2$, and Mn_2I_4(18-crown-6) even outperform long-optimized commer-

https://dx.doi.org/10.1021/jacs.0c09454
J. Am. Chem. Soc. 2021, 143, 798−804

cial phosphors with unprecedented quantum yields of 82, 98, and 100% at ambient temperature. This excellent PL performance can be directly correlated to the structural features of the respective compounds. Besides bright PL, Mn_2I_4(18-crown-6) shows an anisotropic angle-dependent emission under polarized light and a second-order nonlinear optical effect, which can be again related to its structural features with finite, noninversion symmetric sensitizer–activator Mn^{2+}–Mn^{2+} couples and the presence of a polar, chiral space-group symmetry ($P2_12_12_1$). Such optical properties with bright emission, quantum yields near unity, and NLO effects (including polarized emission, SHG, and visible emission via SHG-driven excitation) are surprising and observed for the first time.

■ ASSOCIATED CONTENT

Supporting Information

The Supporting Information is available free of charge at https://pubs.acs.org/doi/10.1021/jacs.0c09454.

Details related to the synthesis, crystal structure analysis, spectroscopic characterization, computation, and techniques related to the nonlinear optical effects (PDF)

X-ray crystallographic data of **1** (CIF)

X-ray crystallographic data of **2** (CIF)

X-ray crystallographic data of **3** (CIF)

X-ray crystallographic data of **4** (CIF)

X-ray crystallographic data of **5** (CIF)

X-ray crystallographic data of **6** (CIF)

X-ray crystallographic data of **7** (CIF)

X-ray crystallographic data of **8** (CIF)

X-ray crystallographic data of **9** (CIF)

X-ray crystallographic data of **10** (CIF)

X-ray crystallographic data of **11** (CIF)

■ AUTHOR INFORMATION

Corresponding Author

Claus Feldmann − *Institute of Inorganic Chemistry (IAC), Karlsruhe Institute of Technology (KIT), D-76131 Karlsruhe, Germany;* orcid.org/0000-0003-2426-9461; Email: claus.feldmann@kit.edu

Authors

Elena Merzlyakova − *Institute of Inorganic Chemistry (IAC), Karlsruhe Institute of Technology (KIT), D-76131 Karlsruhe, Germany*

Silke Wolf − *Institute of Inorganic Chemistry (IAC), Karlsruhe Institute of Technology (KIT), D-76131 Karlsruhe, Germany*

Sergei Lebedkin − *Institute of Nanotechnology (INT), Karlsruhe Institute of Technology (KIT), 76344 Eggenstein-Leopoldshafen, Germany*

Lkhamsuren Bayarjargal − *Institute of Geosciences, Goethe University Frankfurt, D-60438 Frankfurt am Main, Germany*

B. Lilli Neumeier − *Institute of Inorganic Chemistry (IAC), Karlsruhe Institute of Technology (KIT), D-76131 Karlsruhe, Germany*

Daniel Bartenbach − *Institute of Inorganic Chemistry (IAC), Karlsruhe Institute of Technology (KIT), D-76131 Karlsruhe, Germany*

Christof Holzer − *Institute of Physical Chemistry, Karlsruhe Institute of Technology (KIT), D-76131 Karlsruhe, Germany;* orcid.org/0000-0001-8234-260X

Wim Klopper − *Institute of Nanotechnology (INT) and Institute of Physical Chemistry, Karlsruhe Institute of Technology (KIT), 76344 Eggenstein-Leopoldshafen, Germany;* orcid.org/0000-0002-5219-9328

Bjoern Winkler − *Institute of Geosciences, Goethe University Frankfurt, D-60438 Frankfurt am Main, Germany;* orcid.org/0000-0001-8029-478X

Manfred Kappes − *Institute of Nanotechnology (INT) and Institute of Physical Chemistry, Karlsruhe Institute of Technology (KIT), 76344 Eggenstein-Leopoldshafen, Germany;* orcid.org/0000-0002-1199-1730

Complete contact information is available at: https://pubs.acs.org/10.1021/jacs.0c09454

Notes

The authors declare no competing financial interest.

■ ACKNOWLEDGMENTS

C.F. gratefully thanks the Deutsche Forschungsgemeinschaft (DFG) for funding in the Priority Program SPP1708 "Synthesis near room temperature". W.K. and M.K. thank the DFG for funding in the Collaborative Research Center TRR 88 "3MET".

■ REFERENCES

(1) (a) Pedersen, C. Cyclic Polyethers and Their Complexes with Metal Yalts. *J. Am. Chem. Soc.* **1967**, *89*, 7017–7036. (b) Bradshaw, J. S.; Izatt, R. M. A.; Bordunov, V.; Zhu, C. Y.; Hathaway, J. K.; Gokel, G. W. Crown ethers. *Comprehensive Supramolecular Chemistry* **1996**, *1*, 35–95. (c) Liu, Z.; Nalluri, S. K. M.; Stoddart, J. F. Surveying Macrocyclic Chemistry: From Flexible Crown Ethers to Rigid Cyclophanes. *Chem. Soc. Rev.* **2017**, *46*, 2459–2478.

(2) Fabbrizzi, L. *Cryptands and Cryptates*; World Scientific: Hackensack, NJ, 2018.

(3) Dye, J. L. Electrides: Early Examples of Quantum Confinement. *Acc. Chem. Res.* **2009**, *42*, 1564–1572.

(4) Shirakawa, S.; Maruoka, K. Recent Developments in Asymmetric Phase-Transfer Reactions. *Angew. Chem., Int. Ed.* **2013**, *52*, 4312–4348.

(5) Smith, J. M.; Sadique, A. R.; Cundari, T. R.; Rodgers, K. R.; Lukat-Rodgers, G.; Lachicotte, R. J.; Flaschenriem, C. J.; Vela, J.; Holland, P. L. Studies of Low-Coordinate Iron Dinitrogen Complexes. *J. Am. Chem. Soc.* **2006**, *128*, 756–769.

(6) Steed, J. W. First- and Second-sphere Coordination Chemistry of Alkali Metal Crown Ether Complexes. *Coord. Chem. Rev.* **2001**, *215*, 171–221.

(7) (a) Paul, I.; Mittal, N.; De, S.; Bolte, M.; Schmittel, M. Catch-Release System for Dosing and Recycling Silver(I) Catalyst with Status of Catalytic Activity Reported by Fluorescence. *J. Am. Chem. Soc.* **2019**, *141*, 5139–513. (b) Jarolimova, Z.; Vishe, M.; Lacour, J.; Bakker, E. Potassium Ion-Selective Fluorescent and pH Independent Nanosensors Based on Functionalized Polyether Macrocycles. *Chem. Sci.* **2016**, *7*, 525–533. (c) Takashima, I.; Kanegae, A.; Sugimoto, M.; Ojida, A. Aza-Crown-Ether-Appended Xanthene: Selective Ratiometric Fluorescent Probe for Silver(I) Ion Based on Arene-Metal Ion Interaction. *Inorg. Chem.* **2014**, *53*, 7080–7082. (d) Li, Y. P.; et al. Ratiometric and Selective Fluorescent Sensor for Zn^{2+} as an "Off-On-Off" Switch and Logic Gate. *Inorg. Chem.* **2012**, *51*, 9642–9648. (e) Fages, F.; Desvergne, J. P.; Bouas-Laurent, H.; Lehn, J. M.; Konopelski, J. P.; Marsau, P.; Barrans, Y. Synthesis and Fluorescence Emission Properties of a Bisanthracenyl Macrotricyclic Ditopic Receptor. Crystal structure of Its Dinuclear Rubidium Cryptate. *J. Chem. Soc., Chem. Commun.* **1990**, 655–658.

(8) Valeur, B.; Leray, I. Design Principles of Fluorescent Molecular Sensors for Cation Recognition. *Coord. Chem. Rev.* **2000**, *205*, 3−40.
(9) (a) Xemard, M.; Cordier, M.; Molton, F.; Duboc, C.; Le Guennic, B.; Maury, O.; Cador, O.; Nocton, G. Divalent Thulium Crown Ether Complexes with Field-Induced Slow Magnetic Relaxation. *Inorg. Chem.* **2019**, *58*, 2872−2880. (b) Starynowicz, P. Two Complexes of Sm(II) with Crown Ethers - Electrochemical Synthesis, Structure and Spectroscopy. *Dalton Trans.* **2004**, 825−832. (c) Starynowicz, P. Europium(II) Complexes with Unsubstituted Crown Ethers. *Polyhedron* **2003**, *22*, 337−345. (d) Adachi, G.-Y.; Sorita, K.; Kawata, K.; Tomokiyo, K.; Shiokawa, J. Luminescence of Divalent Europium Complexes with 18-crown-6 Derivatives. *Inorg. Chim. Acta* **1985**, *109*, 117−121. (e) Bunzli, J. C. G.; Klein, B.; Chapuis, G.; Schenk, K. J. Diffusion of Cadmium Acetate and Self-diffusion of Cadmium Ions in Cadmium Acetate in Agar Gel Medium. *Inorg. Chem.* **1982**, *21*, 808−810.
(10) de Mello, J. C.; Wittmann, H. F.; Friend, R. H. An Improved Experimental Determination of External Photoluminescence Quantum Efficiency. *Adv. Mater.* **1997**, *9*, 230−232.
(11) Wasserscheid, P.; Welton, T. *Ionic Liquids in Synthesis*; Wiley-VCH: Weinheim, 2008.
(12) Shannon, R. D. Revised Effective Ionic Radii and Systematic Studies of Interatomic Distances in Halides and Chalcogenides. *Acta Crystallogr., Sect. A: Cryst. Phys., Diffr., Theor. Gen. Crystallogr.* **1976**, *A32*, 751−767.
(13) Hausmann, D.; Kuzmanoski, A.; Feldmann, C. $MnBr_2$/18-crown-6 Coordination Complexes Showing High Room Temperature Luminescence and Quantum Yield. *Dalton Trans.* **2016**, *45*, 6541−6547.
(14) (a) Suffren, Y.; O'Toole, N.; Hauser, A.; Jeanneau, E.; Brioude, A.; Desroches, C. Discrete Polynuclear Manganese(II)complexes with Thiacalixarene Ligands: Synthesis, Structures and Photophysical Properties. *Dalton Trans.* **2015**, *44*, 7991−8000. (b) Chekhlov, A. N. Synthesis and Crystal Structure of Bis[(18-crown-6)oxonium]-tetrabromomanganese(II). *Russ. J. Gen. Chem.* **2008**, *78*, 1862−1865. (c) Fender, N. S.; Fronczek, F. R.; John, V.; Kahwa, I. A.; McPherson, G. L. Unusual Luminescence Spectra and Decay Dynamics in Crystalline Supramolecular $[(A1_8C_6)_4MBr_4][TlBr_4]_2$ (A = Rb, K; M = 3d Element) Complexes. *Inorg. Chem.* **1997**, *36*, 5539−5547.
(15) (a) Junk, P. C.; Smith, M. K.; Steed, J. W. Anion-induced Structural Diversity in 12-crown-4 Complexes of Transition Metal Salts. *Polyhedron* **2001**, *20*, 2979−2988. (b) Doxsee, K. B.; Hagadorn, H. R.; Weakley, T. J. R. Metal- vs Hydrogen-Bonding Complexation in Zinc Complexes of 18-Crown-6. *Inorg. Chem.* **1994**, *33*, 2600−2606. (c) Bel'skii, V. K.; Strel'tsova, N. R.; Bulychev, B. M.; Storozhenko, P. A.; Ivankina, L. V.; Gorbunov, A. I. Complexation of Metal Salts with Macrocyclic Polyethers in Aprotic Solvents. Crystal Structures of Ionic $[Zn{\cdot}15\text{-crown-}5{\cdot}2L]^{2+}[Zn_2Cl_6]^{2-}$ (L = CH_3CN, THF), $[ZnCl{\cdot}15\text{-crown-}5{\cdot}L']^{2+}[Zn_2Cl_6]^{2-}$ (L' = H_2O, CH_3COCH_3) and Molecular $ZnCl_2{\cdot}18\text{-crown-}6{\cdot}H_2O$ and $ZnCl_2{\cdot}2CH_3CN$ Complexes. *Inorg. Chim. Acta* **1989**, *164*, 211−220.
(16) (a) Atwood, J. L.; Junk, P. C. Formation and Crystal Structures of Novel Seven-coordinate 15-crown-5 Complexes of Manganese(II), Iron(II) and Cobalt(II). *Polyhedron* **2000**, *19*, 85−91. (b) Reid, H. O. N.; Kahwa, I. A.; White, A. J. P.; Williams, D. J. Seven-coordinate Mn^{2+} Ions in $[Mn(15\text{-crown-}5)(H_2O)_2]^{2+}$ as Luminescent Probes for Dynamic Supramolecular Events. *Chem. Commun.* **1999**, 1565−1566. (c) Deng, Y.; Burns, J. H.; Moyer, B. A. Complexation of Manganese(II) by Cyclohexano-15-crown-5 in Propylene Carbonate: Calorimetric and X-ray Crystallographic Investigation. *Inorg. Chem.* **1995**, *34*, 209−213.
(17) (a) Shionoya, S.; Yen, W. M.; Yamamoto, H. *Phosphor Handbook*; CRC Press: Boca Raton, FL, 2006. (b) Blasse, G.; Grabmeier, B. C. *Luminescent Materials*; Springer: Berlin, 1994.
(18) (a) Zeuner, M.; Pagano, S.; Schnick, W. Nitridosilicates and Oxonitridosilicates: From Ceramic Materials to Structural and Functional Diversity. *Angew. Chem., Int. Ed.* **2011**, *50*, 7754−7775. (b) Pust, P.; Weiler, V.; Hecht, C.; Tücks, A.; Wochnik, A. S.; Henß, A.-K.; Wiechert, D.; Scheu, C.; Schmidt, P. J.; Schnick, W. Narrow-band Red-emitting $Sr[LiAl_3N_4]:Eu^{2+}$ as a Next-generation LED-phosphor Material. *Nat. Mater.* **2014**, *13*, 891−896.
(19) (a) Pallavi, P.; Kumar, V.; Hussain, W.; Patra, A. Excited-State Intramolecular Proton Transfer-Based Multifunctional Solid-State Emitter: A Fluorescent Platform with "Write-Erase-Write" Function. *ACS Appl. Mater. Interfaces* **2018**, *10*, 44696−44705. (b) Bestgen, S.; Schoo, C.; Neumeier, B. L.; Feuerstein, T. J.; Zovko, C.; Köppe, R.; Feldmann, C.; Roesky, P. W. Intensely Photoluminescent Diamidophosphines of the Alkaline-Earth Metals, Aluminum, and Zinc. *Angew. Chem., Int. Ed.* **2018**, *57*, 14265−14269. (c) Ding, Y.; Li, X.; Li, T.; Zhu, W.; Xie, Y. α-Monoacylated and α,α'- and α,β'-Diacylated Dipyrrins as Highly Sensitive Fluorescence "Turn-on" Zn^{2+} Probes. *J. Org. Chem.* **2013**, *78*, 5328−5338.

https://dx.doi.org/10.1021/jacs.0c09454
J. Am. Chem. Soc. 2021, 143, 798−804